Steady nonlinear capillary waves on curved sheets

DARREN CROWDY

Department of Mathematics, Imperial College of Science, Technology and Medicine,
180 Queen's Gate, London SW7 2BZ, UK
email: d.crowdy@ic.ac.uk

This paper presents a new class of solutions for steady nonlinear capillary waves on a curved sheet of fluid in the plane. The solutions are exact in that the free surfaces of the sheet and the associated flow field can be found in closed form. The solutions are generalizations of the classic solutions for finite amplitude waves on fluid sheets [5] to the case where the fluid sheets are curved.

1 Introduction

The study of irrotational flows involving free capillary surfaces is a fluid dynamical problem of classical interest. Lord Rayleigh [9] studied the effects of capillarity on jets of fluid although his investigations were restricted to infinitesimal waves. In a recent paper, Crowdy [2] described a new mathematical approach to the study of finding *finite amplitude* solutions to free surface problems involving Euler flows with surface tension and retrieved the classic exact results of Crapper [1] and Kinnersley [5] using a method which is general enough in scope to produce many other classes of exact solutions to related problems [3, 4].

This paper presents a new class of solutions for steady nonlinear capillary waves on a curved sheet of fluid in the plane. These are obtained by generalizing some recently-derived exact solutions for steady capillary waves on an annulus of fluid [4]. The solutions are intimately related to the classic exact solutions for waves on fluid sheets derived by Kinnersley [5] and indeed can be viewed as finite amplitude capillary waves on fluid sheets which are not 'straight' (as in Kinnersley's case) but 'curved'.

The principal purpose of this paper is to present a new class of non-trivial exact solutions to a highly nonlinear free boundary problem, variants of which have received much attention in the literature. Only a few other exact solutions to this class of problems are known besides those of Crapper [1], Kinnersley [5] and Crowdy [2, 14, 4]. In 1955, McLeod [7] found an isolated exact solution for a bubble in a uniform flow, while Longuet-Higgins [6] lists several other special cases. The solutions presented here represent a rare example of exact solutions to a free boundary problem involving *two* interacting free surfaces (the fluid regions considered here are doubly-connected and are bounded by two disjoint free surfaces).

We are not currently aware of any physical problem in which the solutions in the geometry considered here might have any direct application, so we concentrate here on

presenting the mathematical solutions as an example of the use of complex variable methods in the study of free boundary problems. Given the highly nonlinear nature of the problem, we feel that it is important to document any known exact solutions. The fact that the solutions are non-trivial means that they can provide important benchmarks for checking numerical codes designed to analyse problems where additional physical effects are introduced and exact results not available. Note also that the equations solved here are isomorphic to those relevant to the magnetic shaping of molten metal columns [10] – an important paradigmatic problem in various industrial continuous casting processes. Indeed, shapes of molten metal columns displaying qualitatively similar features to those presented in this paper are computed numerically in Shercliff [10]. Our exact solutions will also serve as benchmark solutions in that rather separate application.

2 Mathematical formulation

To obtain solutions for steady capillary waves on curved sheets, we proceed by supposing that the sheet 'closes' so that it forms a region of fluid swirling in an annular configuration. The problem of steady capillary waves on a fluid annulus has previously been considered in Crowdy [4], where it is shown that the problem admits a (continuous) two-parameter family of exact solutions. In what follows, it is shown that the solutions of Crowdy [4] are just the first in a discrete infinity of such two-parameter families of exact solutions. This generalization is important in that it results in a class of solutions to the problem of capillary waves on fluid annuli which are much more diverse and flexible than those already presented in Crowdy [4]. For example, by taking suitable choices of parameters in the solutions presented here, it turns out that we can generate solutions for capillary waves on very thin fluid annuli and, in §4, we consider just half such an annulus (which still constitutes a global equilibrium of the equations) as a model of a planar fluid 'jet' in equilibrium under the effects of surface tension. We point out that the exact solutions presented in Crowdy [4] did not permit any solutions of this kind (i.e. solutions involving very thin annuli). In addition, the solutions of Crowdy [4] correspond to situations in which the coefficients of surface tension on the two free boundaries are rather different. The generalized solutions herein include classes of solution where the ratio of the surface tension coefficients can draw very close to unity – a much more physically-realistic scenario.

Introduce a conformal map $z(\zeta)$ from the annulus $\rho < |\zeta| < 1$ in a parametric ζ-plane to the fluid annulus (see Figure 1). For convenience, the annulus $\rho < |\zeta| < 1$ will be referred to as C_0. Because it will be needed later in the analysis, the annulus $1 < |\zeta| < \rho^{-1}$ is denoted C_1. The circle $|\zeta| = 1$ is taken to map to the outer interface of the fluid annulus while $|\zeta| = \rho$ maps to the inner interface.

The flow is assumed to be irrotational so that a complex potential $w(z)$ can be introduced in the usual way. Define the composite function

$$W(\zeta) = w(z(\zeta)). \tag{2.1}$$

For steady equilibrium, the kinematic condition that the two boundaries of the annulus
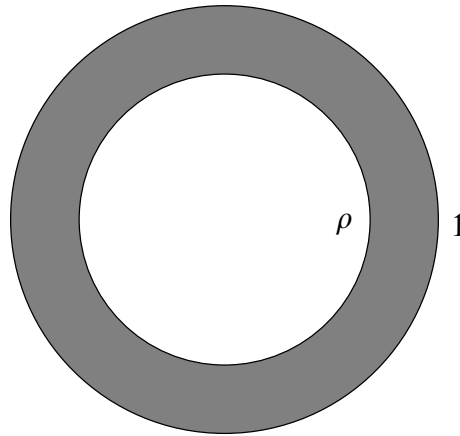
FIGURE 1. Parametric ζ-plane.

are streamlines can be written as

$$\psi \equiv \text{Im}[W(\zeta)] = \text{const.} \tag{2.2}$$

on $|\zeta| = \rho$ and $|\zeta| = 1$. In what follows, we seek a class of solutions in which this complex potential is given by the special form

$$W(\zeta) = i\gamma \log \zeta, \tag{2.3}$$

for some real constant γ, which will represent a measure of how fast the fluid is swirling in the annulus. Note that (2.3) satisfies (2.2). The dynamic boundary condition states that on each interface the fluid pressure is balanced by the surface tension, i.e.

$$\begin{aligned} p - p_1 &= T_1 \kappa, & \text{on } |\zeta| = 1; \\ p - p_\rho &= -T_\rho \kappa, & \text{on } |\zeta| = \rho, \end{aligned} \tag{2.4}$$

where κ is the interface curvature, and p_1 and p_ρ represent the fluid pressure outside the fluid annulus and in the enclosed bubble, respectively, and T_1 and T_ρ are the respective (constant) coefficients of surface tension. Bernoulli's Theorem states that the dynamic pressure of the fluid p is given by

$$p + \frac{1}{2} \left| \frac{dw}{dz} \right|^2 = H, \tag{2.5}$$

where H is a constant. Nondimensionalizing the equations for the dynamic boundary conditions using T_1, on $|\zeta| = 1$, the Bernoulli pressure conditions can be rewritten in the form

$$-\frac{d}{d\zeta} \left[\frac{\zeta z_\zeta(\zeta)}{\zeta^{-1} \bar{z}_\zeta(\zeta^{-1})} \right]^{1/2} + \Gamma_1 z_\zeta = \frac{W_\zeta(\zeta) \overline{W}_\zeta(\zeta^{-1})}{2 \bar{z}_\zeta(\zeta^{-1})}, \tag{2.6}$$

while on $|\zeta| = \rho$ it takes the form

$$\beta \frac{d}{d\zeta} \left[\frac{\zeta z_\zeta(\zeta)}{\rho^2 \zeta^{-1} \bar{z}_\zeta(\rho^2 \zeta^{-1})} \right]^{1/2} + \Gamma_\rho z_\zeta = \frac{W_\zeta(\zeta) \overline{W}_\zeta(\rho^2 \zeta^{-1})}{2 \bar{z}_\zeta(\rho^2 \zeta^{-1})}. \tag{2.7}$$

β denotes the ratio of the surface tension coefficients on each interface

$$\beta \equiv \frac{T_\rho}{T_1}. \tag{2.8}$$

Γ_1 and Γ_ρ are constants which can be interpreted as governing the value of the constant fluid pressures outside and inside the fluid annulus respectively. In a physical situation, differences in the values of the surface tension parameters might be due to the presence of different types/concentrations of surfactants on each interface or due to differences in temperature inside and outside the annulus. Perhaps most physically useful, however, is the case where both interfaces have the *same* coefficient of surface tension and we will later show that for the 'thin' annuli within the class of solutions considered here, the value of β can draw very close to unity.

To construct solutions, we follow the method presented in detail in Crowdy [4]. First define the function $S(\zeta)$ to be a nonlinear function of $z_\zeta^{1/2}$ and its conjugate function $\bar{z}_\zeta^{1/2}$ by

$$S(\zeta) \equiv -\frac{d}{d\zeta} \left[\frac{\zeta z_\zeta(\zeta)}{\zeta^{-1}\bar{z}_\zeta(\zeta^{-1})} \right]^{1/2} + \Gamma_1 z_\zeta. \tag{2.9}$$

In Theorem 3.1 of Crowdy [4], it is established that if, for given Γ_1 and γ^2, a conformal map satisfying conditions (i)–(iv) below can be found, then a solution to the original free boundary problem has been found. The four conditions are:

(i) $z(\zeta)$ is a univalent conformal map from C_0 to the fluid region;

(ii) $[z_\zeta]^{1/2}$ satisfies the functional equation

$$[z_\zeta(\rho^2\zeta)]^{1/2} = \Omega \ [z_\zeta(\zeta)]^{1/2}, \tag{2.10}$$

where Ω is some real, negative constant (to be determined);

(iii) $[z_\zeta]^{1/2}$ is meromorphic in C_1 with only simple pole singularities;

(iv) $S(\zeta)$ is analytic everywhere in C_1 and satisfies the equation

$$S(1) = \frac{\gamma^2}{2\bar{z}_\zeta(1)}. \tag{2.11}$$

These results are stated here without proof and the interested reader is referred to Crowdy [4] for more complete details. If the solutions are such that the square root of the derivative of the conformal map satisfies the functional relation (2.10) then in order for (2.6) and (2.7) to be consistent, it is necessary that β and Γ_ρ be given by the following algebraic equations:

$$\beta = -\frac{1}{\Omega\rho},$$
$$\frac{\Gamma_1}{\Gamma_\rho} = \rho^2\Omega^2. \tag{2.12}$$

Because β must be positive, it is clear from (2.12) that only solutions in which Ω is *real* and *negative* are physically admissible.

3 Exact solutions

We now use the conditions (i)–(iv) in a *constructive* way to produce solutions. Condition (iii) dictates that $[z_\zeta]^{1/2}$ has only simple pole singularities in C_1 so we attempt to seek a solution in which $[z_\zeta]^{1/2}$ has a finite number $N \geqslant 2$ of simple poles where N is some integer. Solutions in the special case $N = 2$ have already been found in Crowdy [4], where the question of the existence of solutions in which $N > 2$ was left open. We now demonstrate by explicit construction that such solutions exist. The new solutions correspond to solutions in which each interface has an order-N rotational symmetry. The question of existence of solutions *without* such symmetry is not addressed here and remains open. The constructive methods of Crowdy [4] are, it is emphasized, still applicable to solutions without symmetry.

Because we seek solutions with rotational symmetry, we expect the singularities and zeros of the derivative of the conformal map to be distributed in the complex plane with the same rotational symmetry. To exploit this symmetry maximally, it is convenient to define two functions $P_N(\zeta; \rho)$ and $Q_N(\zeta; \rho)$ via the infinite product expansions:

$$P_N(\zeta; \rho) = (1 - \zeta^N) \prod_{k=1}^{\infty} (1 - \rho^{2kN}\zeta^N)(1 - \rho^{2kN}\zeta^{-N}), \tag{3.1}$$

$$Q_N(\zeta; \rho) = (1 + \zeta^N) \prod_{k=1}^{\infty} (1 + \rho^{2kN}\zeta^N)(1 + \rho^{2kN}\zeta^{-N}). \tag{3.2}$$

These functions are analytic everywhere in the complex ζ-plane except at zero and infinity. It can be shown by direct manipulation of these infinite product expansions that $P_N(\zeta)$ and $Q_N(\zeta)$ satisfy the functional equations:

$$P_N(\zeta^{-1}) = P_N(\rho^2\zeta) = -\frac{1}{\zeta^N}P_N(\zeta),$$

$$Q_N(\zeta^{-1}) = Q_N(\rho^2\zeta) = \frac{1}{\zeta^N}Q_N(\zeta). \tag{3.3}$$

Now define the derivative of a conformal map by

$$z_\zeta(\zeta) = \hat{R}\left(\frac{Q_N(\frac{\zeta}{\alpha\zeta_1}); \rho)}{P_N(\frac{\zeta}{\zeta_1}); \rho)}\right)^2, \tag{3.4}$$

where $\alpha, \hat{R}$ and ζ_1 are real constants and where $1 < \zeta_1 < \rho^{-1}$ while α is assumed to be positive. Consider the singularity structure of this map in the annulus C_1. The function (3.4) has N second-order poles at points in C_1 all having modulus ζ_1 and with arguments of the Nth roots of unity. Similarly, this function has precisely N zeros in C_1 all having modulus $\alpha\zeta_1$ (it will be assumed that α is such that $1 < \alpha\zeta_1 < \rho^{-1}$) and with arguments of the Nth roots of -1.

It remains to find α. For any given ζ_1, ρ and $\hat{R}$, the constant α is chosen so that it is a *real* solution of the nonlinear algebraic equation given by

$$\text{Residue}[z_\zeta(\zeta); \zeta_1] = 0, \tag{3.5}$$

where the notation denotes the residue of $z_\zeta(\zeta)$ at $\zeta = \zeta_1$. This equation is clearly

independent of $\hat{R}$, but appears to depend upon all three of the remaining parameters ζ_1, ρ and N. In fact, solutions to this equation turn out to be independent of ζ_1, but depend only on ρ and N. This fact is most easily seen in the case when $\rho = 0$ (corresponding to a simply-connected blob of fluid containing a line vortex – see Crowdy [3] for more details of this problem) where it can be shown that the solution of (3.5) for α is

$$\alpha = \left(\frac{N+1}{N-1} \right)^{1/N}. \tag{3.6}$$

In the general case, α is a function of ρ and N, i.e. $\alpha = \alpha(\rho, N)$. The analytical solution (3.6) will be used later to check the results of a Newton iterative procedure used to calculate solutions for α when $\rho \neq 0$.

Now define an auxiliary function $\hat{P}_N(\zeta; \rho)$ via the infinite product expansion

$$\hat{P}_N(\zeta; \rho) = \prod_{j=1}^{N-1} (1 - \zeta \omega_N^j) \prod_{k=1}^{\infty} (1 - \rho^{2kN} \zeta^N)(1 - \rho^{2kN} \zeta^{-N}), \tag{3.7}$$

where $\omega_N = e^{\frac{2\pi i}{N}}$. Then, for any given ζ_1, ρ and $\hat{R}$ (with α given as a real solution of (3.5)) we set Γ_1 to be given by the formula

$$\Gamma_1 = \frac{\hat{P}_N(1; \rho)}{\hat{R} Q_N(\alpha^{-1}; \rho) \bar{z}_\zeta^{1/2}(\zeta_1^{-1})}, \tag{3.8}$$

and we set γ^2 to be given by

$$\gamma^2 = 2\bar{z}_\zeta(1)S(1). \tag{3.9}$$

Note that both quantities Γ_1 and γ^2 are *real*, as required. Provided (3.5) and (3.8) are satisfied, it can be shown that the composite function $S(\zeta)$ is *analytic* at all the poles of z_ζ in C_1, i.e. the two conditions (3.5) and (3.8) together imply that the principal part of $S(\zeta)$ at $\zeta_1 \omega_N^j$, $j = 0, 1, \ldots, N-1$ vanishes. This is a necessary condition for solution because $S(\zeta)$ must be analytic at these points (see condition (iv) above). Using the properties (3.3), it can further be shown that (3.4) satisfies the functional equation (2.10) with the choice

$$\Omega = -\alpha^N. \tag{3.10}$$

If α is *real* and *positive* (as supposed above) then Ω is *real* and *negative* as required for a physically admissible solution. (We note in passing that functions satisfying the multiplicative property (2.10) in the case where $\Omega = 1$ are known as *loxodromic functions* and the present analysis is based on ideas and generalizations of the general theory of such functions. For a general discussion of loxodromic functions see Valiron [13] and a useful appendix in Richardson [8]). Next, provided that γ^2 is given by the formula (3.9) then (2.11) will be satisfied, as also required for a consistent solution to the problem (see condition (iv) above). Finally, given Γ_1 and γ^2, the relevant values of β and Γ_ρ then follow from (2.12).

We have now constructed a conformal map satisfying all the (necessary and sufficient) conditions (ii)–(iv) for a consistent solution to the original problem. It only remains to check condition (i), i.e. that the primitive of (3.4) is a *univalent* conformal map from C_0 to the annular fluid domain. Even if all the above equations can be solved for a given ζ_1 and

ρ, this final requirement may not hold and the solution for such a choice of parameters ζ_1 and ρ will therefore be physically inadmissible.

3.1 Primitive of (3.4)

To check for univalency of the mapping function and to actually plot the two interfaces, it is necessary to integrate (3.4) to find $z(\zeta)$. Remarkably, a closed-form formula can be found for the primitive of (3.4). Consider the conformal map $z(\zeta)$ given by

$$z(\zeta) = R\zeta \frac{P_N(\frac{\zeta}{\alpha^2 \zeta_1}); \rho)}{P_N(\frac{\zeta}{\zeta_1}); \rho)}, \tag{3.11}$$

where R is a real constant which is not independent of α, ζ_1 and R but is given by the equation

$$\hat{R} = -R\left(\frac{P_N(\alpha^{-2}; \rho)P'_N(1; \rho)}{[Q(\alpha^{-1}; \rho)]^2}\right), \tag{3.12}$$

where $P'_N(\zeta; \rho)$ denotes the derivative of $P_N(\zeta; \rho)$ with respect to ζ. (3.11) is an analytical expression for the primitive of (3.4).

Irrespective of the details of the method of construction of the solutions, the fact that the formulae just obtained represent solutions of the original physical problem can be verified *directly* by substitution of the exact formulae into the boundary conditions (2.6)–(2.7). This was done (using `Mathematica`) as an explicit check on the solutions.

3.2 Summary of the exact solutions

Provided the area of the fluid annulus is specified, a continuous two parameter family of exact solutions has thus been found for each integer $N \geqslant 2$. The solutions are most conveniently parametrized by ζ_1 and ρ. The conformal map from C_0 is given by (3.11). The parameter α is determined as the real solution to (3.5) (provided such a solution exists). The constant R can be determined (as a function of ζ_1, ρ and N) by (arbitrarily) specifying the area of the blob to be π, i.e. by imposing that

$$\pi = \frac{1}{2}\text{Im}\left[\oint_{|\zeta|=1} \bar{z}(\zeta^{-1})z_\zeta(\zeta)d\zeta - \oint_{|\zeta|=\rho} \bar{z}(\rho^2\zeta^{-1})z_\zeta(\zeta)d\zeta\right]. \tag{3.13}$$

Given ζ_1, ρ and N, and with R and α determined in the way just described, the corresponding Γ_1 and γ^2 are given by the formulae (3.8) and (3.9). Γ_ρ and β then follow from (2.12) and (3.10).

4 Discussion of solutions

In Figure 2 the solution of (3.5) for $\alpha(\rho, N)$ as a function of ρ for $N = 3, 4$ and 10 are plotted. These graphs are obtained by solving the nonlinear equation (3.5) using Newton's method. In the limit $\rho \to 0$ the solutions are given by (3.6) as expected. The range of ρ plotted in these graphs is approximately the range for which physically admissible
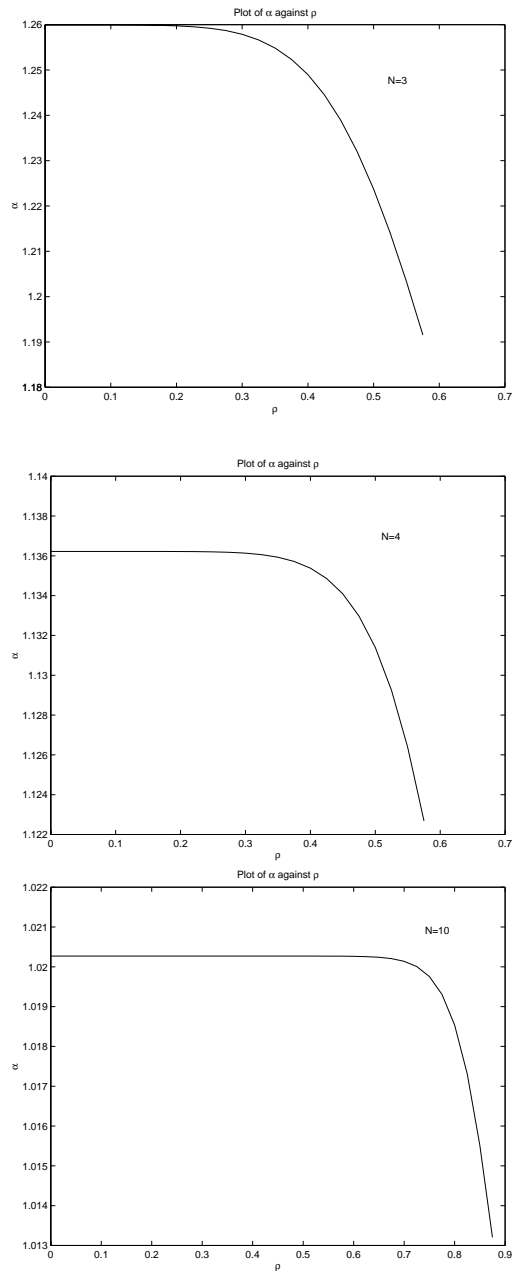
FIGURE 2. Graphs of α against ρ for $N = 3, 4, 10$.

solutions exist – note that for given N, there appears to be a maximum value of ρ for which (3.11) gives a univalent mapping (for any value of ζ_1). It is found that for fixed N, as ρ increases towards unity, the set of ζ_1-values for which solutions exist decreases in size until it eventually becomes empty. It is also found that, for fixed ρ, as N increases the size of the interval of ζ_1 for which solutions exist increases.
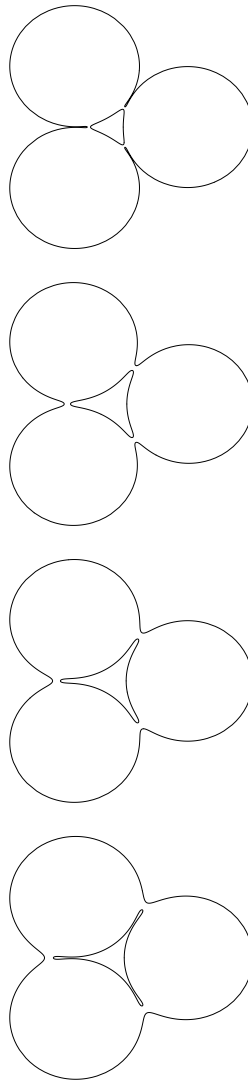
FIGURE 3. $N = 3, \rho = 0.5; \zeta_1 = 1.07, 1.15, 1.20, 1.24.$

Some typical shapes of the fluid annulus are plotted in Figures 3–5 as ζ_1 is altered for fixed $\rho = 0.5$ in the cases $N = 3, 4$ and 10. It is found in general that for a given N and ρ, there exists a range of ζ_1 values for which physically admissible solutions exist. To 2 decimal places, the ranges of existence for $\rho = 0.5$ and $N = 3, 4$ and 10 are found to be

$$\zeta_1 \in [1.07, 1.24] \qquad (N = 3),$$
$$\zeta_1 \in [1.09, 1.43] \qquad (N = 4), \qquad (4.1)$$
$$\zeta_1 \in [1.06, 1.81] \qquad (N = 10).$$

As is evident from the shapes in Figures 3–5, the cause of breakdown of the solutions at either end of this range of existence for ζ_1 is interesting: for ζ_1 at the lower end of the range of existence, solutions break down due to loss of univalency of the conformal

D. Crowdy
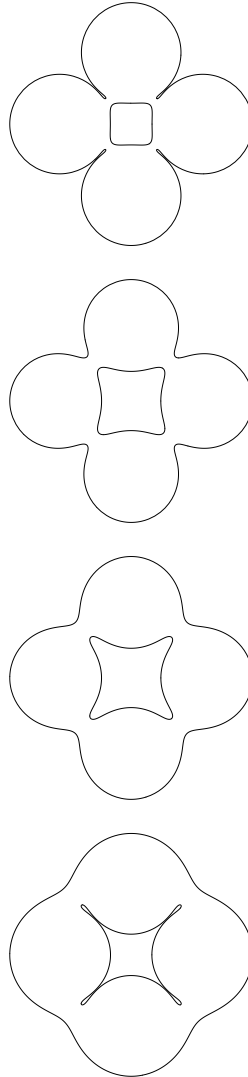
FIGURE 4. $N = 4$, $\rho = 0.5$; $\zeta_1 = 1.09$, 1.20, 1.30, 1.435.

map in the *outer* interface, while for ζ_1-values at the upper end of the range of existence, breakdown is due to loss of univalency of the mapping in the *inner* interface. In all cases calculated, loss of univalency occurs because separate parts of the *same* interface draw together in an *N*-symmetric formation to enclose *N* small constant pressure bubbles – a phenomenon analogous to the formation of an enclosed bubble at a critical wave-speed in Crapper's classic exact solution [1] for steady capillary waves on deep water. Note that, in all cases calculated, it is never found that breakdown is due to the two *different* interfaces coming into contact. We also note that, as might be expected, the shape of the enclosed bubbles (inside the fluid annulus) exhibit the same qualitative features as observed in the calculations of a constant pressure bubble situated in an ambient circulatory swirling flow of infinite extent as studied in Crowdy [3] and Wegmann & Crowdy [14].
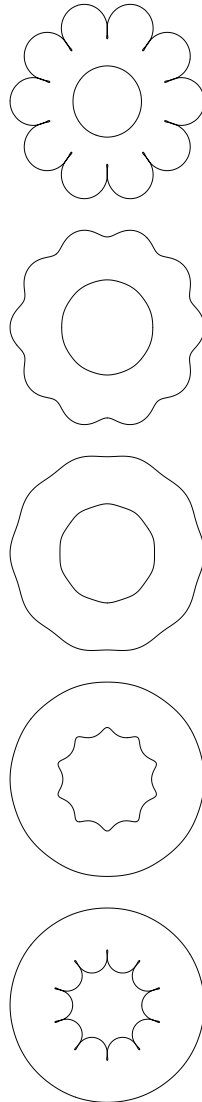
FIGURE 5. $N = 10, \rho = 0.5$; $\zeta_1 = 1.06$, 1.20, 1.30, 1.65, 1.81.

Figure 6 shows graphs of $\frac{\Gamma_1}{\Gamma_\rho}$ and $\frac{T_1}{T_\rho}$ (i.e. β^{-1}) as functions of ρ for $N = 3$, 4 and 10. An important observation is that as $\rho \to 1^-$, both ratios get closer to unity. As $\rho \to 1^-$, in general the annuli become thinner so that physically this result means that *thinner* annuli of this kind can support equilibria where the surface tension coefficients and pressures on either side of the sheet are commensurate. This important point is discussed again later.

In Figures 7–12, graphs of Γ_1 and γ^2 are plotted as functions of ζ_1 for $\rho = 0.5$ and $N = 3, 4$ and 10. In the case $N = 3$, the graph of γ^2 is monotone increasing throughout the range of existence of solutions while for $N = 4$ and $N = 10$ it is found that the graphs of both Γ_1 and γ^2 have turning points at some critical ζ_1 within the range of existence of solutions (although not, in general, at the same critical value of ζ_1). The turning points in
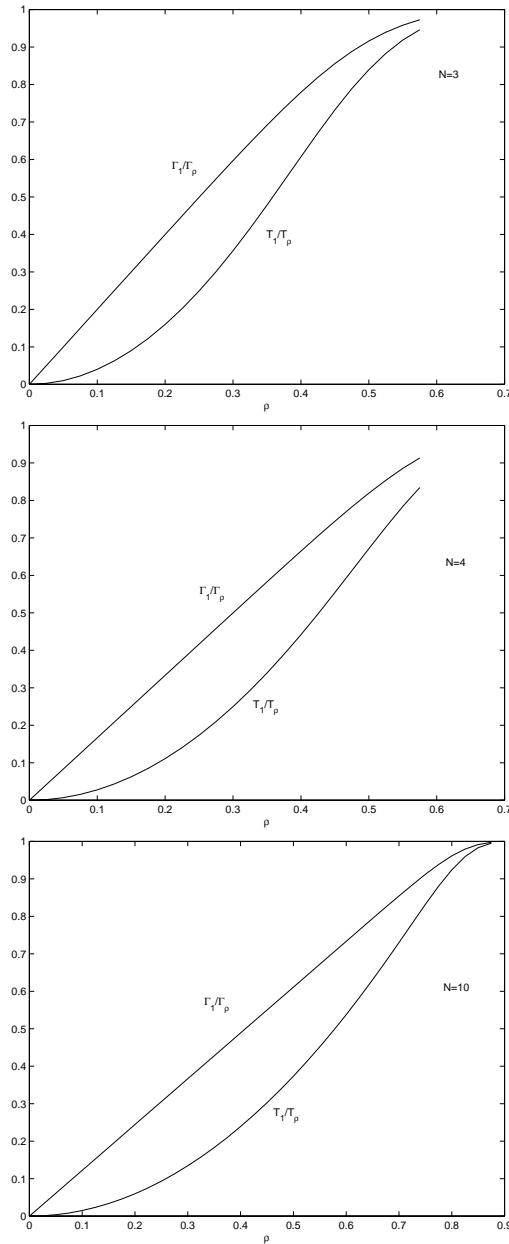
FIGURE 6. Graphs of $\frac{\Gamma_1}{\Gamma_\rho}$ and $\frac{T_1}{T_\rho}$ against ρ for $N = 3$, 4, 10.

the graphs of γ^2 suggest a non-uniqueness in the specification of solutions. For example, it is physically sensible to specify the parameters β and γ^2. Specifying the surface tension ratio β is essentially equivalent, via equation (2.12), to specifying ρ. Specifying γ^2 can be considered equivalent to specifying a pole position ζ_1. However, the graphs show that for a specified γ^2 there appears to exist *two* distinct equilbrium shapes (for a fluid annulus
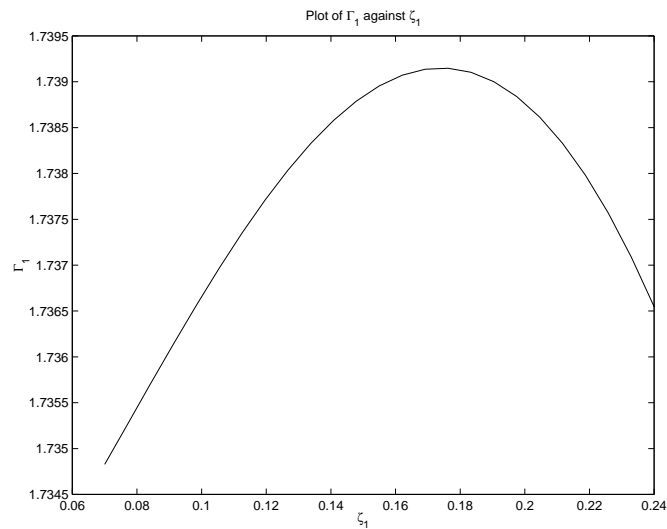
Plot of Γ_1 against ζ_1

FIGURE 7. Graph of Γ_1 against ζ_1 for $\rho = 0.5$, $N = 3$.

Plot of γ^2 against ζ_1
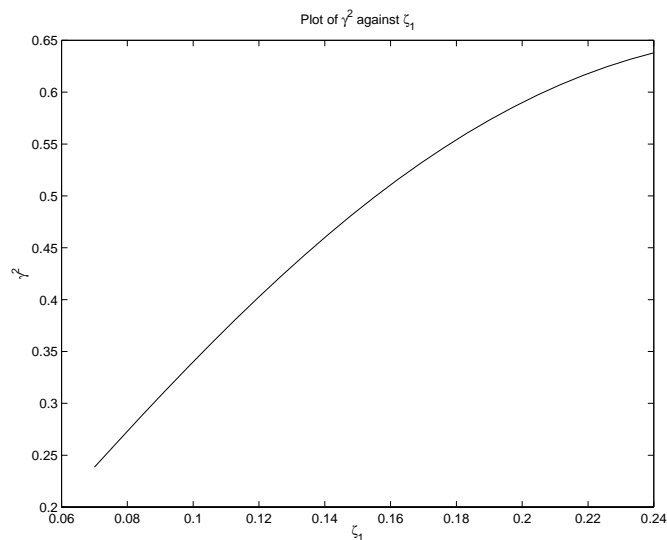
FIGURE 8. Graph of γ^2 against ζ_1 for $\rho = 0.5$, $N = 3$.

of area π) with any given order of rotational symmetry $N \geqslant 4$. Each of these two shapes has its own value of Γ_1.

Finally, in Figures 13–15 some typical streamlines inside the fluid annulus are shown. In these diagrams the innermost and outermost streamlines (shown in bold) are the boundaries of the fluid annulus.

Plot of Γ_1 against ζ_1

FIGURE 9. Graph of Γ_1 against ζ_1 for $\rho = 0.5$, $N = 4$.

Plot of γ^2 against ζ_1
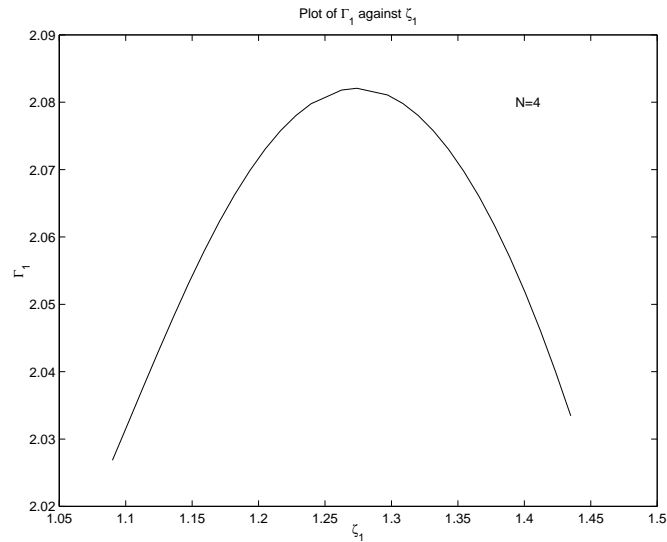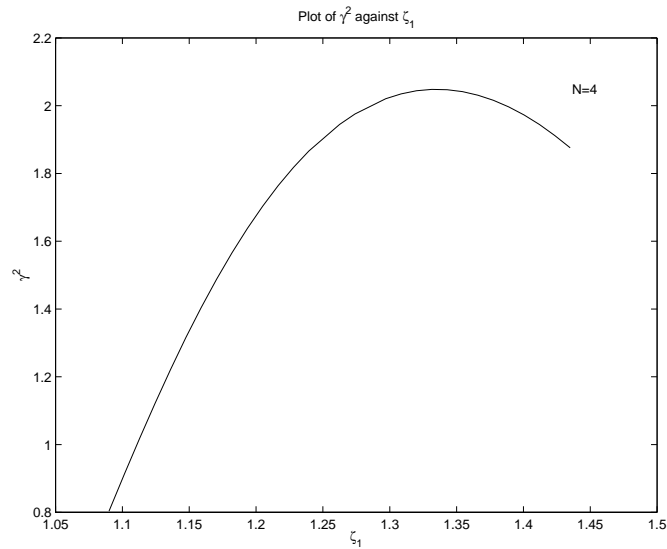
FIGURE 10. Graph of γ^2 against ζ_1 for $\rho = 0.5$, $N = 4$.

4.1 Solutions with $\rho = 0$

In the case $\rho = 0$ we obtain exact solutions to a rather different physical problem in which an irrotational swirling flow is induced in a *simply-connected* blob of fluid by a line vortex singularity actually situated inside the droplet of fluid. This particular mathematical problem was considered in Crowdy [3] as a model of circulation-induced shape deformations in free drops and exact solutions found corresponding to the case
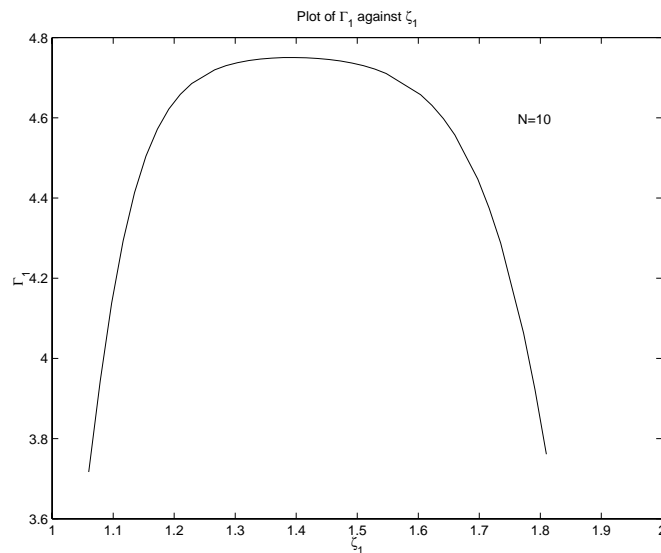
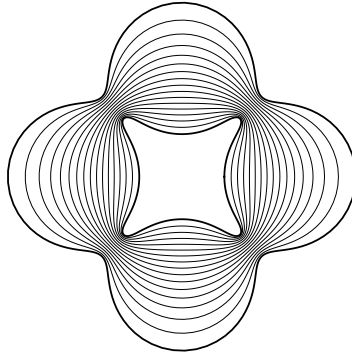FIGURE 11. Graph of Γ_1 against ζ_1 for $\rho = 0.5$, $N = 10$.
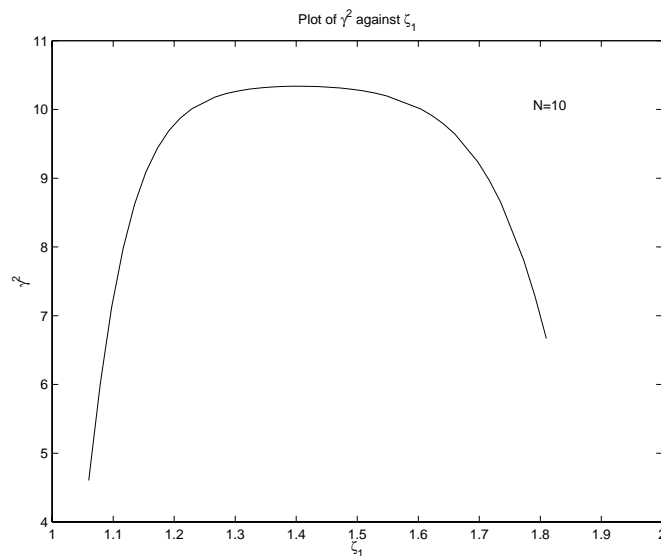
FIGURE 12. Graph of γ^2 against ζ_1 for $\rho = 0.5$, $N = 10$.

$N = 2$. The question of existence of solutions to this problem for $N > 2$ was left open in Crowdy [3]. Taking $\rho = 0$ in the solutions above provides an affirmative (and constructive) answer to this open question of existence. Exact solutions to this problem exist for all integers $N \geqslant 2$.

FIGURE 13. Typical streamlines: $N = 4$, $\rho = 0.5$, $\zeta_1 = 1.3$.
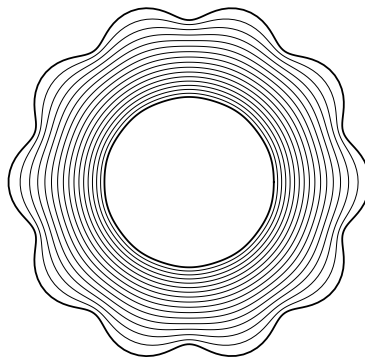
FIGURE 14. Typical streamlines: $N = 10$, $\rho = 0.5$, $\zeta_1 = 1.2$.
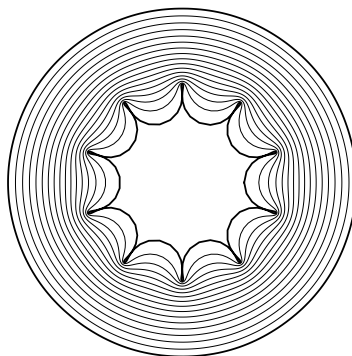
FIGURE 15. Typical streamlines: $N = 10$, $\rho = 0.5$, $\zeta_1 = 1.81$.
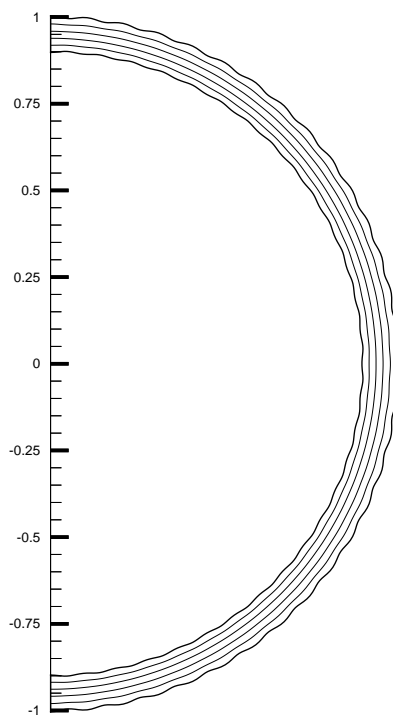
FIGURE 16. Streamlines of thin curved jet: $N = 60, \rho = 0.9, \zeta_1 = 1.05$.

4.2 Curved jets: $\rho \to 1^-$

In the limit as $\rho \to 1^-$, the width of the fluid annulus becomes small. In this limit, the solutions just found can be interpreted as 'curved sheets of fluid' or 'curved jets' in the plane. We note here that a well-known example of curved sheets of fluid in equilibrium where the effects of surface tension are important is the phenomenon known as a 'water bell' [11, 12].

If we take N large in the solutions just obtained and plot only 'half' a fluid annulus (so that the solutions more closely resemble 'jets' of fluid) then it turns out to be possible to find solutions in which ρ gets close to unity and produces solutions for relatively thin jets of fluid. Two example plots for the cases $N = 60$ and $N = 100$ are shown in Figures 16 and 17. The solutions shown in Figures 16 and 17 appear to be very close to the geometrically trivial case of two concentric circles forming a thin annulus of fluid. Indeed, such a configuration is perhaps a more obvious solution to the problem of a steady, thin, curved planar jet with capillarity. Such a geometrically trivial configuration is indeed a possible equilibrium solution of the governing equations. In this case, the relevant conformal map
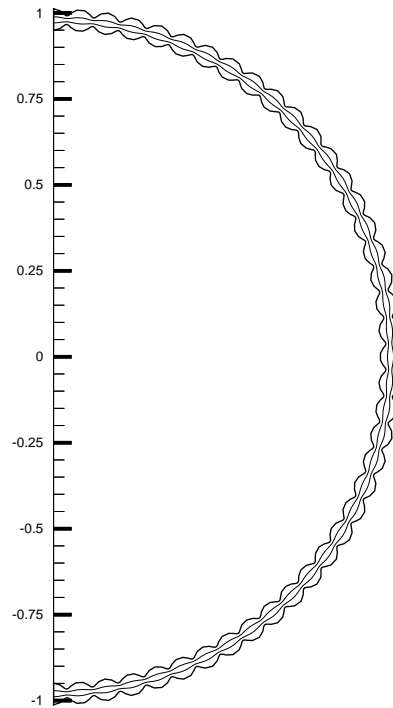
FIGURE 17. Streamlines of thin curved jet: $N = 100, \rho = 0.97, \zeta_1 = 1.015$.

from C_0 is simply $z(\zeta) = \zeta$. The two dynamic boundary conditions require that

$$-1 + \Gamma_1 = \frac{\gamma^2}{2},$$
$$\frac{\beta}{\rho} + \Gamma_\rho = \frac{\gamma^2}{2\rho^2}. \tag{4.2}$$

These equations imply

$$\Gamma_1 - \rho^2 \Gamma_\rho = 1 + \beta\rho, \tag{4.3}$$

so that in the case where the surface tension coefficients on the two interfaces are the same (i.e. $\beta = 1$) and the thickness of the annulus gets very small (i.e. $\rho \to 1^-$) then

$$\Gamma_1 - \Gamma_\rho \to 2, \tag{4.4}$$

i.e. the two constant pressure regions on either side of the thin jet must have different pressures if the annulus is to be in equilibrium.

On the other hand, for certain choices of the parameters, the geometrically nontrivial
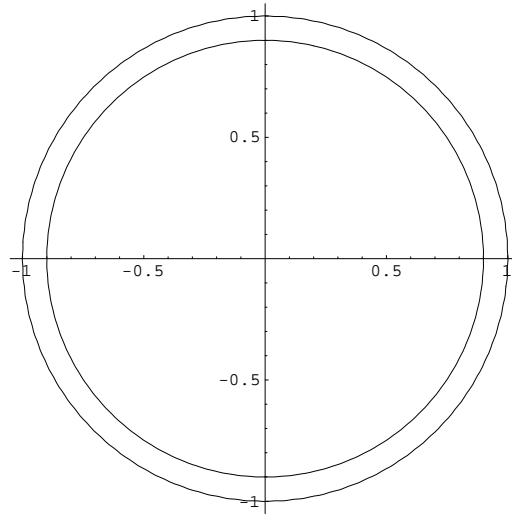
FIGURE 18. Conformal map (3.11) for $N = 80, \rho = 0.9, \zeta_1 = 1.05$: the shape is virtually indistinguishable from two concentric circles of radii 0.9 and 1.0.

solutions just obtained become indistinguishably close to the annulus $\rho < |\zeta| < 1$ in the limit as $N \to \infty$. In Figure 18 we plot the conformal map (3.11) for the choice $N = 80, \rho = 0.9$ and $\zeta_1 = 1.05$. The resulting shape is virtually indistinguishable (at least within a 'picture norm') from the trivial case of an annulus consisting of two concentric circles of radius 0.9 and 1. Note the crucial point, however, that the curvature of the interfaces in the nontrivial solutions (in Figure 18, for example) is not constant (as in the annulus case consisting of two concentric circles), but is such that the ratios $\frac{\Gamma_1}{\Gamma_\rho}$ and $\frac{T_1}{T_\rho}$ are relatively close to unity. That this happens in general as N gets large is clear from the graphs in Figure 6. Specifically, for the curved jet solution illustrated in Figure 16 for the parameter values $N = 60, \rho = 0.9$ and $\zeta_1 = 1.05$ the corresponding value of $\frac{T_1}{T_\rho}$ (correct to 2 decimal places) is 0.93 while $\frac{\Gamma_1}{\Gamma_\rho} = 0.87$ (correct to 2 d.p.) while in Figure 17, which shows the case where $N = 100, \rho = 0.97, \zeta_1 = 1.015$, the corresponding values are $\frac{T_1}{T_\rho} = 0.99$ and $\frac{\Gamma_1}{\Gamma_\rho} = 0.98$ (to 2 d.p.) which are very close to unity.

The new solutions therefore seem to provide more satisfactory mathematical models for planar fluid jets in equilibrium under the effects of surface tension than the trivial concentric annulus solution. It might be concluded from our results that capillary waves are a *necessary* feature for force balance on the surface of a thin fluid jet if it is to form a steady structure on both sides of which the ambient pressures are commensurate.

5 Final remarks

Kinnersley [5] identified a class of 'symmetric' and 'anti-symmetric' waves on *straight* fluid sheets which have no global radius of curvature (as in the solutions found here). As discussed in Crowdy [4], the solutions here are the natural analogues of the 'symmetric' class of waves in Kinnersley [5]. It is likely (although, in a nonlinear problem of this kind, by no means guaranteed) that there also exist analogues of the anti-symmetric solutions in the case of curved fluid sheets. To find such solutions, allowance must be made for

a possible 'phase shift' in the two surface waves. To incorporate this mathematically, it might be more convenient to adopt an approach using elliptic function conformal maps from a fundamental parallelogram in the spirit of Kinnersley's original analysis. We have not yet succeeded in finding any such anti-symmetric analogues for waves on fluid annuli.

The question of the linear stability of the new solutions is clearly important but requires detailed numerical investigation and is beyond the scope of the present paper. Another question is whether this problem admits any classes of unsteady, *time-evolving* exact solutions. Such solutions might help in understanding the problem of inviscid capillary pinch-off. Preliminary investigations show this to be unlikely, although research continues into this interesting possibility.

References

[1] Crapper, G. D. (1957) An exact solution for progressive capillary waves of arbitrary amplitude. *J. Fluid Mech.*, **2**, 532–540.

[2] Crowdy, D. G. (2000) A new approach to free surface Euler flows with surface tension. *Stud. Appl. Math.*, **105**, 35.

[3] Crowdy, D. G. (1999) Circulation-induced shape deformations of drops and bubbles: exact two-dimensional models. *Phys. Fluids*, **11**(10), 2836–2845.

[4] Crowdy, D. G. (1999) Exact solutions for capillary waves on a fluid annulus. *J. Nonlin. Sci.*, **9**, 615–640.

[5] Kinnersley, W. (1977) Exact large amplitude capillary waves on sheets of fluid. *J. Fluid Mech.*, **77**, 229–241.

[6] Longuet-Higgins, M. S. (1988) Limiting forms of capillary-gravity waves. *J. Fluid Mech.*, **194**, 351.

[7] McLeod Jr., E. B. (1955) The explicit solution of a free boundary problem involving surface tension. *J. Rat. Mech. Anal.*, **4**, 557.

[8] Richardson, S. (1996) Hele-Shaw flows with time-dependent free boundaries involving a concentric annulus. *Phil. Trans. Roy. Soc. Lond. A*, **353**, 2513.

[9] Rayleigh, Lord (1879) On the capillary phenomena of jets. *Proc. Roy. Soc.*, **29**, 71–97.

[10] Shercliff, J. A. (1981) Magnetic shaping of molten metal colunms. *Proc. Roy. Soc. Lond.*, **375**, 455.

[11] Taylor, G. I. (1953) The dynamics of thin sheets of fluid I; water bells. *Proc. Roy. Soc. Lond.*, **253**, 289–295.

[12] Taylor, G. I. (1953) The dynamics of thin sheets of fluid II; waves on fluid sheets. *Proc. Roy. Soc. Lond.*, **253**, 296–312.

[13] Valiron, G. (1947) *Cours d'Analyse Mathematique: Theorie des Fonctions*, 2nd Ed. Masson et Cie, Paris.

[14] Wegmann, R. & Crowdy, D. G. (2000) Shapes of two-dimensional bubbles deformed by circulation. *Nonlinearity*, **13**, 2131.